

Cotunneling and one-dimensional localization in individual single-wall carbon nanotubes

B. Gao,¹ D.C. Glattli,^{1,2} B. Plaças,¹ A. Bachtold^{1,3*}
¹ *Laboratoire Pierre Aigrain, Ecole Normale Supérieure,*
24 rue Lhomond, 75231 Paris 05, France. ² *SPEC, CEA Saclay,*
F-91191 Gif-sur-Yvette, France, ³ *ICN and CNM-CSIC,*
Campus UABarcelona, E-08193 Bellaterra, Spain.
 (Dated: February 15, 2019)

We report on the temperature dependence of the intrinsic resistance of long individual disordered single-wall carbon nanotubes. The resistance grows dramatically as the temperature is reduced, and the functional form is consistent with an activated behavior. These results are described by Coulomb blockade along a series of quantum dots. We occasionally observe a kink in the activated behavior that reflects the change of the activation energy as the temperature range is changed. This is attributed to charge hopping events between non-adjacent quantum dots, which is possible through cotunneling processes.

PACS numbers: 73.63.Fg, 73.20.Fz, 73.23.Hk

Single-wall carbon nanotubes (SWNT) are an excellent system to study one-dimensional (1-d) transport. In particular, the effect of disorder in 1-d is very pronounced; current lines have to follow the wire and cannot go round impurity centers. As the transmission of impurity centers becomes low enough, the 1-d wire is divided in a series of quantum dots. The conduction is then thermally activated $R(T) \approx \exp(T^{-1})$ [1, 2, 3, 4].

Measurements on 2-d or 3-d arrays of quantum dots can show a slower than thermally activated dependence of the conduction $R(T) \approx \exp(T^{-0.5})$ [5, 6]. This has been recently attributed to cotunneling processes, which allow charge transfer between non-adjacent quantum dots [7, 8, 9]. Indeed, cotunneling transport in a series of quantum dots is analogous to variable-range hopping (VRH) [10]. Charges try to find hopping events with the lowest activation energy and the shortest hopping distance. The slower than thermally activated dependence of the conduction is then a result of successive thermally activated curves with the activation energy that decreases as the temperature is reduced. However, such a succession of activated curves remain to be observed.

Localization experiments have been carried on nanotube films or individual SWNTs contacted to microfabricated electrodes, but tube-tube junctions and tube-electrode interfaces make the analysis difficult [4, 11, 12, 13, 14]. In our experiments, the intrinsic resistance of disordered SWNTs is measured in a four-point configuration [15]. The intrinsic resistance is found to be thermally activated. As the gate voltage (V_g) is swept, we observe Coulomb blockade oscillations that can be rather regular in some cases. These measurements are consistent with a series of quantum dots that are typically $\gtrsim 10$ nm long. Importantly, we also observe kinks in the activated behavior of $R(T)$ that suggest the change of the activation energy as the temperature range is varied. These kinks are attributed to cotunneling processes.

The fabrication of SWNT devices for four-point mea-

| | L (nm) | L_e (nm) | E_0 (meV) | L_{dot} (nm) | |
|----------|----------|------------|-------------|----------------|-------|
| Device 1 | 1370 | 18 | 13.0 | ~ 50 | SC |
| Device 2 | 780 | 29 | 7.6 | ~ 90 | metal |
| Device 3 | 1640 | 20 | 9.3 | ~ 75 | metal |
| Device 4 | 1000 | 27 | 11.5 | ~ 60 | metal |
| Device 5 | 590 | 300 | | | metal |

TABLE I: Device characteristics. L is the length between the MWNTs. L_{dot} is calculated from E_0 extracted at $V_g = 0$. SC = semiconducting tube with the threshold voltage at ~ 40 V.

surements has been described in Ref. [15]. Briefly, ~ 1 nm diameter SWNTs grown by laser-ablation [16] are selected with an atomic force microscopy (AFM). Noninvasive voltage electrodes are defined by positioning two MWNTs above the SWNT using AFM manipulation. Cr/Au electrodes are patterned for electric connection using electron-beam lithography (Fig. 1(a)). Characteristics of the devices are summarized in Table 1.

The four-point resistance R_{4pt} of some SWNTs is particularly large > 100 k Ω at 300 K. The nature of the scattering centers responsible for this resistance is at present not understood. Figure 1(b) shows the temperature dependence of R_{4pt} of one of those SWNTs (device 1). The curve is quite flat at high T , while the resistance increases a lot below 100 K. The high-temperature resistance allows the estimation of the elastic mean-free path L_e . Using $R_{4pt} = h/4e^2 \cdot L/L_e$ with L the length between the MWNTs [15], we get $L_e = 18$ nm.

For comparison, we also show a device that is significantly less resistive at 300 K, $R_{4pt} = 12$ k Ω . The $R_{4pt}(T)$ variation is much less pronounced. This is consistent with previously reported works on two-point, low ohmic SWNT devices, where the $R_{2pt}(T)$ dependence is weak [17, 18, 19]. For two-point devices with a large resistance, the resistance has been reported to strongly grow as T goes to zero, which is usually associated to the change of the contact resistance [20]. In our case, the four-point

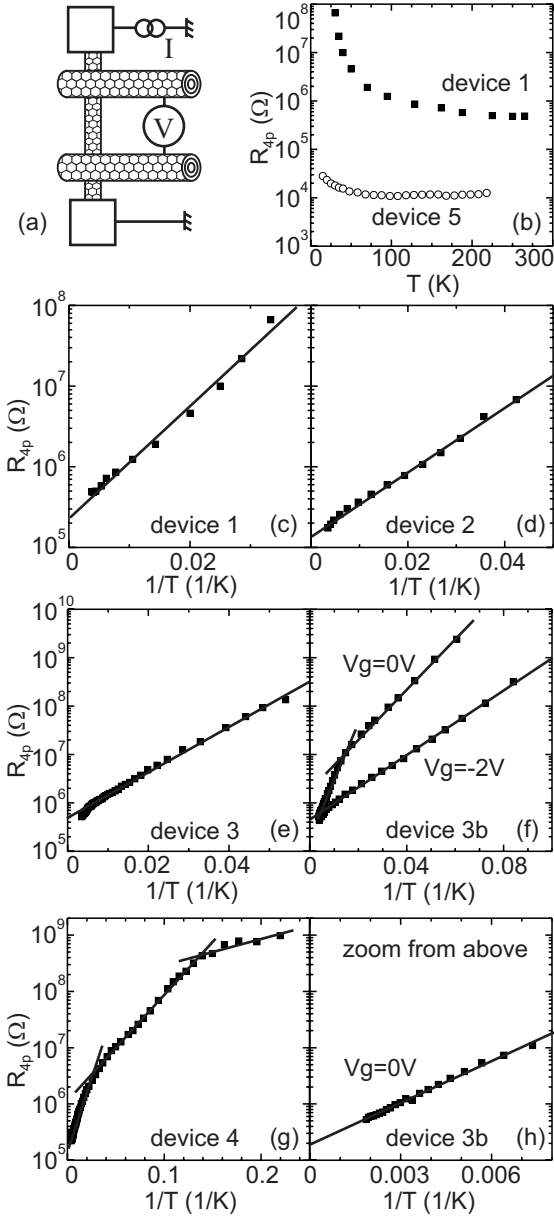


FIG. 1: Four-point resistance. (a) Device schematic. (b-h) R_{4pt} as a function of temperature. When the value of V_g is not indicated, $V_g = 0$. Device 3b is the same device as Device 3, but it has been measured one month before. Microscopic changes might have been occurred in between.

technique allows to separate the intrinsic and contact resistances.

Figure 1(c) shows that the above measurement in the highly diffusive tube is consistent with an activated behavior of the resistance

$$R_{4pt} = R_0 \exp \frac{E_0}{kT} \quad (1)$$

with E_0 the activation energy. This dependency is observed in other devices (see Fig. 1(d-f)). Similar $R(T)$

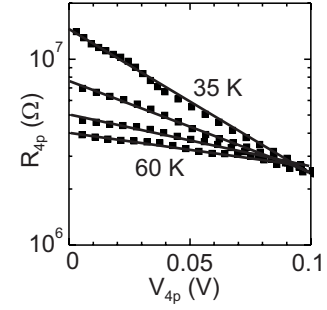


FIG. 2: Four-point differential resistance as a function of V_{4pt} for Device 1 at 35, 45, 55, and 60 K.

behaviors have been reported for disordered wires micro-fabricated in semiconductors [21, 22].

Figures 1(f-h) show $R(T)$ measurements on other tubes. Some of them deviate from the standard activated behavior. However, these measurements can be described by successive exponential functions with different activation energies, giving rise to kinks. Interestingly, Fig. 1(f) shows that those two exponential functions can merge in a single one on varying the gate voltage, which is applied on the back side of the Si wafer. Overall, these measurements suggest that the activation energy depends on the temperature range and the gate voltage.

Further insight into transport properties is obtained by studying the high-voltage regime. Figure 2 shows that the differential R_{4pt} is lowered as V_{4pt} increases, and that the dependence can be fitted with

$$R_{4pt} = R_0 \exp \frac{E_0 - \alpha e V_{4pt}/2}{kT} \quad (2)$$

This suggests that an increase in the voltage reduces the activation energy. An important point is that the slope deduced from Fig. 2 gives α in Eq. (2) below unity. This means that more than one energy barrier has to be overcome along the tube. A rough estimate of the number of barriers N can be made by taking $N = 1/\alpha$, which assumes identical barriers [21]. In this way we obtain $N \lesssim 20$.

Fig. 3(a) shows the effect of the gate voltage, which controls the position of the Fermi level in the tube. Large fluctuations of $R_{4pt}(V_g)$ develop at low T that look random [22, 23]. At first sight, this may question the activation behavior of $R_{4pt}(T)$ and the kinks discussed above. However, Fig. 3(b) shows that a curve similar to Fig. 1(f) ($V_g = 0$) is found by V_g averaging $R_{4pt}(T)$. Moreover, similar dependencies are observed, albeit with different activation energies, for the minima and maxima of $R_{4pt}(V_g)$ as a function of T . This illustrates the robustness of the activation behavior and the kink for a nanotube with a given Fermi level.

While these fluctuations look random, oscillations can be found that are quite regular within restricted V_g ranges [24]. Fig. 3(c) shows 10 successive oscillations.

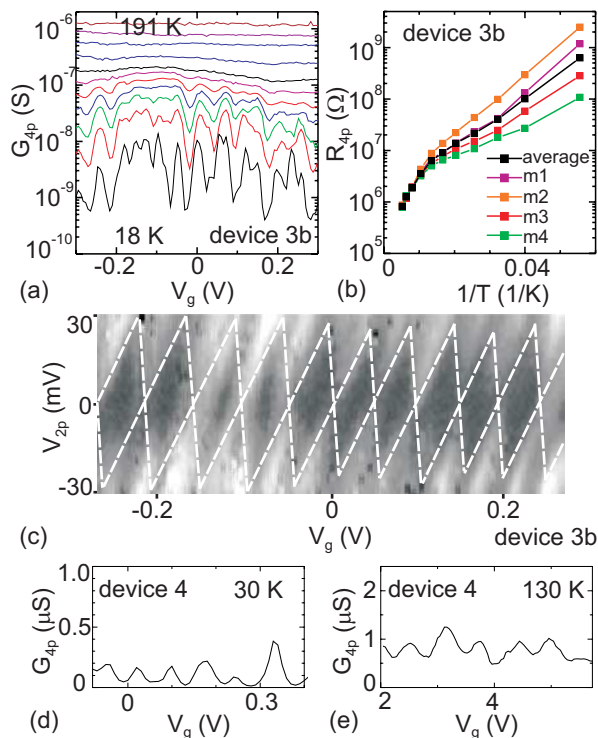


FIG. 3: Four-point resistance as a function of the gate voltage. (a) $R_{4pt}(V_g)$ for Device 3b at 18, 25, 31, 39, 49, 60, 74, 96, 125, 158, and 191 K. (b) $R_{4pt}(T)$ averaged over V_g between -0.3 and 0.3 V and taken at different conductance maxima (m1@0.09V, m2@0.17V, m3@-0.25V, m4@-0.05V). (c) Two-point differential conductance as a function of V_g and V_{2pt} at 20 K. The same measurement with G_{4pt} is very noisy. $R_{4pt}(V_g)$ and $R_{2pt}(V_g)$ in the linear regime show the same features at 20 K. Figures 1(f), 3(a) and 3(c) are taken in three cooling runs. (d,e) $G_{4pt}(V_g)$ for device 4.

Note that series of regular oscillations can be found at other V_g ranges, and the period is then identical. Interestingly, Fig. 3(d,e) show that the period can change as the temperature is modified. New oscillations can appear at lower T that have a shorter period.

We now discuss possible origins for the activated behavior of the resistance. One possible mechanism is the Schottky barrier at the interface between a metal electrode and a semiconducting nanotube [25]. However, we also observe the activated behavior in metal tubes, which have no Schottky barriers. Moreover, the four-point technique is aimed to avoid contributions from the contacts [15]. Another mechanism is thus needed to account for the results.

The fluctuations of $R_{4pt}(V_g)$ and the $R_{4pt}(T)$ dependence may be attributed to universal conductance fluctuations and weak localization. However, the variations of R_{4pt} are much larger than h/e^2 , so that the results cannot simply originate from interference corrections.

Strong localization (SL) is expected for highly diffusive systems [10]. This theory has been used to explain exponential length dependencies of the resistance mea-

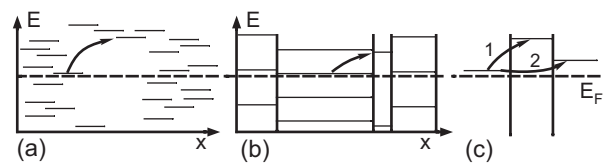


FIG. 4: Schematics of localized states along the nanotube. (a) States are randomly distributed. (b) Strong barriers that define quantum dots. (c) Proposed process to account for the kinks in Fig. 1 (f,g). Arrows represent hopping paths.

sured in nanotubes [26, 27, 28]. SL occurs when the phase-coherence length L_ϕ becomes longer than the localization length L_{loc} . This is equivalent to when the width of the coherent states, $\hbar v_F/L_\phi$, becomes smaller than the energy separation between the localized states. The localized states are usually regarded as randomly distributed in space and energy (see Fig. 4(a)) [29, 30]. Irregular oscillations of $R_{4pt}(V_g)$ are expected, which is in opposition to our results.

We now look at an alternative distribution of localized states as schematized in Fig. 4(b). The tube is here divided in segments separated by highly resistive scattering centers. The segment lengths and therefore the energy separations can be different. At high enough temperatures, levels are thermally smeared out except for the shortest segment that has the largest level separations. Oscillations of $R_{4pt}(V_g)$ are then regular, and the period is large. At lower temperature, shorter periods arise from longer segments, which agrees with experiments.

So far, the Coulomb interaction between electrons has not been taken into account. However, the charging energy E_c of a single nanotube quantum dot is known to be larger than the level spacing ΔE due to the geometrical confinement of the electron wave. $\Delta E \approx 0.5 \text{ meV} \cdot \mu\text{m}$ and the charging energy for a tube dot connected to two tube leads is roughly $E_c \approx 1.4 \text{ meV} \cdot \mu\text{m}$ [31]. This suggests that the separation in energy between the localized states in Fig. 4(b) is given by the charging energy.

Localization related to Coulomb blockade through multiple quantum dots [1, 2, 3, 4] bears a lot in common with the standard hopping model of the strong localization theory [22, 23, 29, 30]. Series of aperiodic conductance oscillations are expected. Contrary to the SL regime, however, quasi-periodic oscillations are also occasionally predicted, in agreement with experiments. In addition the resistance is expected to be thermally activated, which again agrees with experiments. The activation energy is given by the dot with the level that lies the furthest away from the Fermi level. It may also be the largest separation of energy levels located in neighboring dots. Thus, E_0 is expected to be gate voltage dependent, consistent with our experimental findings.

We here estimate the size of the dots. The activation energy E_0 is roughly $0.5E_c$ of the shortest dot. E_0 is 11.5 meV for device 4 at high T . Using $E_c \approx 1.4 \text{ meV} \cdot \mu\text{m}$, we get a dot length of $\sim 60 \text{ nm}$. Another pos-

sibility for this estimation is to use the 625 meV period of the $R_{4pt}(V_g)$ oscillations at high T (Fig. 3(e)). Indeed, $\Delta V_g \approx 12.5$ meV $\cdot\mu\text{m}$ when looking Ref.[31, 32] for a tube dot connected to two tube leads. This gives ~ 20 nm. Note that E_c cannot be estimated from the diamond height in Fig. 3(c) since several dots lie in series. Finally, we obtain ~ 70 nm by dividing the tube length by the dot number obtained in Fig. 2. Those 3 estimations point all to quantum dot lengths of a few 10 nm.

Table 1 gives the dot length of the other samples, estimated from E_0 . Dot lengths are slightly longer than the elastic length L_e determined at 300 K. L_e corresponds to the separation between scatterers when transmissions are 0.5. The barriers that define the quantum dots thus have a transmission $\lesssim 0.5$, which corresponds to a resistance $\gtrsim 6.5$ k Ω . This is consistent with the occurrence of Coulomb blockade since the barrier resistance has to be larger than a few k Ω s.

Having shown that the activated behavior of $R_{4pt}(T)$ originates from a series of quantum dots, we now turn our attention to the kinks (Fig. 1(f-h)). This may simply come from two thermally activated resistances that lie in series. However, the activation energy would be higher at lower T , in opposition to the measurements. Another mechanism is needed to describe the kinks.

We propose that the kink is related to a mechanism that is borrowed from the theory of variable range hopping [10], see Fig. 4(c). Electrons hop to the neighboring quantum dot as indicated by the arrow 1. At lower T it pays to make the hop 2 to the second nearest quantum dot. The activation energy is given by the level separation, which is thus reduced. This is in agreement with the experiments.

In the VHR theory such hops are possible thanks to the tunneling process. However, the tunnel probability is here dramatically low since the second nearest dot is a few tens of nanometers far. Another mechanism for the charge transfer between nonadjacent quantum dots is needed to account for the results.

A possible mechanism is that the charge motion between two nonadjacent dots occurs through cotunneling events [7, 8, 9]. Cotunneling, which involves the simultaneous tunneling of two or more electrons, transfers the charge via a virtual state. This gives rise to current even when the electron transport is Coulomb blocked [33]. A cotunneling event is called inelastic when the quantum dot is left in an excited state, and the event is otherwise called elastic. For an individual quantum dot contacted to two leads, the conductance contribution of elastic cotunneling is temperature independent, while the contribution of inelastic cotunneling scales as T^2 .

Cotunneling in a series of quantum dots has been recently calculated [8, 9]. An energy reservoir supplied by for e.g. phonons is required since ϵ_i the energy of the initial state is most often different than ϵ_f the energy of

the final state (see hop 2 in Fig. 4(c)). The resistance contribution between those two states is [8]

$$R \propto R_0^N \exp \frac{\max(|\epsilon_i - \epsilon_f|, |\epsilon_i - \mu|, |\epsilon_f - \mu|)}{kT} \quad (3)$$

with μ the Fermi level and N the number of dots between the initial and the final states. $R_0 = A_1 E_c / (g \Delta E)$ for elastic cotunneling and $R_0 = A_2 N^2 E_c^2 / (g(\epsilon_i - \epsilon_f)^2)$ for inelastic cotunneling with $g = Gh/e^2$ the average dimensionless conductance of a barrier between two dots and A_1 and A_2 numerical constants of the order of unity. The coulomb repulsion term between the dots i and f is here neglected for simplicity. The prefactor R_0^N grows as N the number of involved barriers gets larger. At high temperature, the hopping process between two adjacent dots dominates transport and the prefactor is low (hop 1 in Fig. 4(c)). As the temperature is reduced, the exponential term grows a lot. It then pays to make the hop between non-adjacent dots when the activation energy is lower (hop 2 in Fig. 4(c)). This is consistent with the kinks observed in Fig. 1.

The temperature T^* of the first kink is expected to be around $kT^* \simeq E_0^{above} - E_0^{below}$ with E_0^{below} and E_0^{above} the activation energies below and above T^* . This can be obtained from Eq. 3 taking into account that $N^{below} - N^{above} = 1$ and that $\ln R_0$ is of the order of unity. This relation is consistent with the experiments. For example, $E_0^{above} - E_0^{below} = 14$ meV in Fig. 1(f) for $V_g = 0$ while $kT^* = 6$ meV.

We have seen that cotunneling processes allow a slower than thermally activated dependence of the conduction. The main contribution of the conduction comes from one (or a few) quantum dot. The energy levels are randomly positioned in energy, so that we cannot expect a specific functional form for the slower than activated dependence measured here.

In conclusion, we have shown that the intrinsic resistance of strongly disordered SWNTs is thermally activated. This is due to Coulomb blockade in a series of $\gtrsim 10$ nm long quantum dots lying along the tube. The activation energy is found to change as the temperature range is changed. We attribute this result to cotunneling processes. Disordered SWNTs form an interesting system for future studies on one-dimensional localization. For example, studies on longer tubes will be investigated to reach the 1-d variable range hopping regime [34].

We thank C. Delalande for support, L. Forro for MWNTs, R. Smalley for laser-ablation SWNTs, and P. McEuen, J.L. Pichard, M. Fogler and M. Feigelman for discussions. LPA is CNRS-UMR8551 associated to Paris 6 and 7. The research has been supported by ACN, Sesame.

* corresponding author: adrian.bachtold@cnm.es

-
- [1] I.M. Ruzin, V. Chandrasekhar, E.I. Levin, and L.I. Glazman, Phys. Rev. B **45**, 13469 (1992).
- [2] A.A.M. Staring, H. van Houten, and C.W.J. Beenakker, Phys. Rev. B **45**, 9222 (1992).
- [3] V. Chandrasekhar, Z. Ovadyahu, and R. A. Webb, Phys. Rev. Lett. **67**, 2862 (1991).
- [4] A. Bezryadin, A.R.M. Verschueren, S.J. Tans, and C. Dekker, Phys. Rev. Lett. **80**, 4036 (1998).
- [5] K.C. Beverly, J.F. Sampaio, J.R. Heath, J. Phys. Chem. B **106**, 2131 (2002).
- [6] D. Yu, C. Wang, B. L. Wehrenberg, and P. Guyot-Sionnest, Phys. Rev. Lett. **92**, 216802 (2004).
- [7] T.B. Tran, I.S. Beloborodov, X.M. Lin, T.P. Bigioni, V.M. Vinokur, and H.M. Jaeger, Phys. Rev. Lett. **95**, 076806 (2005).
- [8] M.V. Feigel'man, A.S. Ioselevich, JETP Lett. **81**, 277 (2005).
- [9] I.S. Beloborodov, A.V. Lopatin, V.M. Vinokur, Phys. Rev. B **72**, 125121 (2005).
- [10] B.I. Shklovskii and A.L. Efros, *Electronic Properties of Doped Semiconductors* (Springer, New York, 1984).
- [11] H.R. Shea, R. Martel, and P. Avouris, Phys. Rev. Lett. **84**, 4441 (2000).
- [12] W. Y. Jang, N.N. Kulkarni, C.K. Shih, and Z. Yao, Appl. Phys. Lett. **84**, 1177 (2004).
- [13] M.S. Fuhrer, M.L. Cohen, A. Zettl and V. Crespi, Solid Stat Commun. **109**, 105 (1998).
- [14] J. Vavro, J.M. Kikkawa, and J.E. Fischer, Phys. Rev. B **71**, 155410 (2005).
- [15] B. Gao, Y.F. Chen, M.S. Fuhrer, D.C. Glatli, and A. Bachtold, Phys. Rev. Lett. **95**, 196802 (2005).
- [16] A. Thess, R. Lee, P. Nikolaev, H. Dai, P. Petit, J. Robert, C. Xu, Y.H. Lee, S.G. Kim, A.G. Rinzler, D.T. Colbert, G.E. Scuseria, D. Tománek, J.E. Fischer, and R.E. Smalley, Science **273**, 483 (1996).
- [17] J. Nygard, D.H. Cobden, P.E. Lindelof, Nature **408**, 6810 (2000).
- [18] W. Liang, M. Bockrath, D. Bozovic, J.H. Hafner, M. Tinkham and H. Park, Nature **411**, 665 (2001).
- [19] J. Kong, E. Yenilmez, T.W. Tomblor, W. Kim, and H. Dai, R.B. Laughlin, L. Liu, C.S. Jayanthi, and S.Y. Wu, Phys. Rev. Lett. **87**, 106801 (2001).
- [20] M. Bockrath, D.H. Cobden, J. Lu, A.G. Rinzler, R.E. Smalley, L. Balents, and P.L. McEuen, Nature **397**, 598 (1999).
- [21] Y.B. Khavin, M.E. Gershenson, and A.L. Bogdanov, Phys. Rev. B **58**, 8009 (1998).
- [22] M.A. Kastner, R.F. Kwasnick, and J.C. Licini, Phys. Rev. B **36**, 8015 (1987).
- [23] A.B. Fowler, A. Hartstein, and R.A. Webb, Phys. Rev. Lett. **48**, 196 (1982).
- [24] S.B. Field, M.A. Kastner, U. Meirav, and J.H.F. Scott-Thomas, D.A. Antoniadis and H.I. Smith, S.J. Wind, Phys. Rev. B **42**, 3523 (1990).
- [25] R. Martel, V. Derycke, C. Lavoie, J. Appenzeller, K.K. Chan, J. Tersoff, and Ph. Avouris, Phys. Rev. Lett. **87**, 256805 (2001).
- [26] P.J. de Pablo, C. Gómez-Navarro, J. Colchero, P.A. Serena, J. Gómez-Herrero, and A.M. Baró, Phys. Rev. Lett. **88**, 036804 (2002).
- [27] J. Cumings, and A. Zettl, Phys. Rev. Lett. **93**, 086801 (2004).
- [28] C. Gómez-Navarro, P.J. de Pablo, J. Gómez-Herrero, B. Biel, F.J. Garcia-Vidal, A. Rubio, and F. Flores, Nature Mat., **4**, 534 (2005).
- [29] Imry, *Electronic Transport in Mesoscopic Systems* (Cambridge University Press, Cambridge, 1997).
- [30] M.M. Fogler and R.S. Kelley, Phys. Rev. Lett. **95**, 166604 (2005).
- [31] D. Bozovic, M. Bockrath, J.H. Hafner, C.M. Lieber, H. Park, and M. Tinkham, Appl. Phys. Lett. **78**, 3693 (2001).
- [32] H.W.C. Postma, T. Teepen, Z. Yao, M. Grifoni, C. Dekker, Science **293**, 76 (2001).
- [33] C. Pasquier, U. Meirav, F.I.B. Williams, and D.C. Glatli, Y. Jin and B. Etienne, Phys. Rev. Lett. **70**, 69 (1993); D.V. Averin and Y.V. Nazarov, *ibid* **65**, 2446 (1990).
- [34] M.M. Fogler, S.V. Malinin, T. Nattermann, cond-mat/0602008.